Hindawi Publishing Corporation
Mathematical Problems in Engineering
Volume 2015, Article ID 258016, 15 pages
http://dx.doi.org/10.1155/2015/258016

Research Article

Effect of Fluctuating Surface Heat and Mass Flux on Natural Convection Flow along a Vertical Flat Plate

Sharmina Hussain,[1] Nepal C. Roy,[2] Md. Anwar Hossain,[2] and Suvash C. Saha[3]

[1]*Department of Mathematics & Natural Sciences, BRAC University, Dhaka 1212, Bangladesh*
[2]*Department of Mathematics, University of Dhaka, Dhaka 1000, Bangladesh*
[3]*School of Physics, Chemistry & Mechanical Engineering, Queensland University of Technology, Brisbane, QLD 4001, Australia*

Correspondence should be addressed to Suvash C. Saha; s_c_saha@yahoo.com

Received 15 August 2015; Accepted 28 October 2015

Academic Editor: Nader Karimi

An investigation has been carried on double diffusive effect on boundary layer flow due to small amplitude oscillation in surface heat and mass flux. Extensive parametric simulations were performed in order to elucidate the effects of some important parameters, that is, Prandtl number, Schmidt number, and Buoyancy ratio parameter on flow field in conjunction with heat and mass transfer. Asymptotic solutions for low and high frequencies are obtained for the conveniently transformed governing coupled equations. Solutions are also obtained for wide ranged value of the frequency parameters. Comparisons between the asymptotic and wide ranged values are made in terms of the amplitudes and phases of the shear stress, surface heat transfer, and surface mass transfer. It has been found that the amplitudes and phase angles obtained from asymptotic solutions are found in good agreement with the finite difference solutions obtained for wide ranged value of the frequency parameter.

1. Introduction

Heat and mass transfer are kinetic processes that may occur in nature, studied separately or jointly. Studying them apart is simpler; however, it is more efficient to consider them jointly. Double diffusive convection creates a buoyancy force so that fluid flow occurs and can be seen in many natural and technological processes. Besides, heat and mass transfer must be jointly considered in some cases like evaporative cooling and ablation. Because of the coupling between the fluid velocity field and the diffusive fields, flow becomes more complicated than the convective flow. Therefore, different behavior may be expected and thus many investigators are still interested in double diffusive flow.

The transport processes due to double diffusion occur in both nature and many engineering applications. Some very important examples of engineering applications include chemical reactions in reactor chamber, chemical vapor deposition of solid layers, combustion of atomized liquid fuels, and dehydration operations in chemical and foundry plants.

An extensive literature survey on this topic has been carried out by Ostrach [1], Huppert and Turner [2], Bejan [3], Gebhart and Pera [4], and Mongruel et al. [5]. Important information and a framework of this type of flow can also be found in the works of these investigators. In their studies, simultaneous heat and mass transfer in buoyancy induced laminar boundary layer flow along a vertical plate have been investigated substantially. Mongruel et al. [5] have proposed a novel method to solve double diffusive boundary layer flow over a vertical flat plate. They considered a vertical flat plate which is immersed in a viscous fluid or in a fluid saturated porous medium. They proposed the integral boundary layer equations and scaling analysis approach. The study of laminar boundary layer flow in presence of an oscillatory potential flow with a steady mean component was first undertaken by Lighthill [6]. He considered the effects of small fluctuations in the free stream velocity on the skin friction and the heat transfer for plates and cylinders by employing the Karman-Pohlhausen approximate integral method. Later, Eshghy et al. [7] and Nanda and Sharma [8] extended Lighthill's theory for

free convection flows. Muhuri and Maiti [9] investigated the free convection flow and heat transfer along a semi-infinite horizontal plate with small amplitude surface temperature oscillation about a nonzero mean, with the same method that has been mentioned. The problem of natural convection flow with an oscillating surface heat flux has been studied by Hossain et al. [10]. The effect of transverse magnetic field on the same type of problem was imposed by Kelleher and Yang [11] and more recently this was also premeditated by Siddiqa et al. [12]. Combined heat and mass transfer above a near-horizontal surface in a fluid saturated media were also studied by Hossain et al. [13]. Less attention has been given to the study of unsteady flow due to double diffusion. Moreover, only the search of similarity solutions has attracted much attention. This is because similarity formulation transforms easily the transport equations into a set of ordinary differential equations which can be solved numerically for different values of the parameters involved. However, some researchers, for example, Khair and Bejan [14] and Trevisan and Bejan [15], set out a framework to solve nonsimilarity solutions for depicting heat and mass transfer with great success. Hossain and Mondal [16] investigated the effect of mass transfer and free convection on the unsteady MHD flow past a vertical plate with constant suction. Later on, the same problem considering variable suction was also investigated by the same authors. Hussain et al. [17] investigated the steady natural convection flow due to combined effects of thermal and mass diffusion from a permeable vertical flat plate. This study focused on the boundary layer regime promoted by the combined events in the permeable surface when the surface is at a nonuniform temperature and a nonuniform mass diffusion but with a uniform rate of suction. Hossain et al. [18] presented the results of unsteady natural convection flow along vertical flat plate subjected to the oscillatory boundary conditions on both surface temperature and species concentration. It has been assumed that both the surface temperature and species concentration have small amplitude temporal oscillations with nonzero means. The mean temperature and mean species concentration are assumed to vary as a power of n of the distance measured from the leading edge. Roy and Hossain [19] studied the effects of conduction-radiation on natural convection flow. In their work, the fluid has been considered as incompressible and unsteady boundary conditions were taken for both surface temperature and mass concentration. Jaman and Hossain [20] presented the results for the flow along a vertical cylinder with elliptic cross section. Hussain [21, 22] focuses on the numerical simulations and analysis of the flow pattern in a spacer-filled flat channel. To find an optimal spacer design, it is essential to determine the flow pattern and turbulence distribution in a spacer-filled channel or spiral-wound module. With the development of more powerful computing techniques, such as computational fluid dynamics (CFD), it has become possible to simulate flow in spacer-filled channels. The basic spacer geometry is modeled as a series of cylindrical filaments partially obstructing the channel. Roy et al. [23] studied the effects of oscillating free stream and surface temperature on natural convection flow along a vertical wedge. In this investigation, the effects of Richardson's number and the Prandtl number have been illustrated. Different numerical techniques are employed to simulate the governing equations and calculated results are compared. Adequate agreement amongst all these calculated values can be noted from these comparisons.

In this present problem, double diffusive flow through a vertical flat plate has been studied extensively. The most important parameter that determines the relative strength of the two buoyancy forces is the ratio parameter w, and, for a positive w, the buoyancy forces are cooperating and drive the flow in the same direction which is considered in this present investigation. This parameter measures the relative importance of solutal and thermal diffusion in causing the density changes which drive the flow. It can be observed that $w = 0$ corresponds to no species diffusion and ∞ to no thermal diffusion. Similar to any double diffusive study, the governing equations of the flow field are simulated for two different diffusive parameters, Pr and Sc. The values of these two parameters depend on the nature of the fluid and on the physical mechanisms governing the diffusion of the heat and chemical species. As the most important fluids are atmospheric air and water, the results are presented here for Pr = 0.7 that represent the air at 20°C at 1 atmosphere against the transpiration parameter ξ and Sc ranged from 0.1 to 1.6. Another important parameter, n, has also been taken into account widely. In this present study, numerical simulations are carried out in detail and results are illustrated in both figures and tabular forms.

2. Formulation of the Problem

A two-dimensional unsteady free convection flow of a viscous incompressible fluid flow along a vertical flat plate in the presence of a soluble species is considered in this present study. It is assumed that both the surface heat flux and surface species concentration flux exhibit small amplitude oscillations in time about a steady nonzero mean temperature and concentration. A semi-infinite vertical flat plate is placed at $y = 0$ in Cartesian coordinate system. And $x \geq 0$, so that the distance from the leading edge along the plate measuring x and y is measured in outward normal direction from the plate. The ambient fluid temperature and species concentration are taken as T_∞ and C_∞. In the case where the surface heat flux and mass flux are considered time dependent, the governing equations of the flow are given by the following sets of Navier-Stokes equations:

$$\begin{aligned}
&\frac{\partial u}{\partial x} + \frac{\partial v}{\partial y} = 0,\\
&\frac{\partial u}{\partial t} + u\frac{\partial u}{\partial x} + v\frac{\partial u}{\partial y} = \nu\frac{\partial^2 u}{\partial y^2} + g\beta_T\left(T - T_\infty\right)\\
&\qquad\qquad + g\beta_C\left(C - C_\infty\right), \qquad (1)\\
&\frac{\partial T}{\partial t} + u\frac{\partial T}{\partial x} + v\frac{\partial T}{\partial y} = \alpha\frac{\partial^2 T}{\partial y^2},\\
&\frac{\partial C}{\partial t} + u\frac{\partial C}{\partial x} + v\frac{\partial C}{\partial y} = D\frac{\partial^2 C}{\partial y^2},
\end{aligned}$$

where u and v are the x and y components of velocity field, respectively, g is the gravitational acceleration, β_T and β_C are the volumetric expansion coefficients for temperature and concentration, respectively, α is the thermal diffusivity, and D is the molecular diffusivity of the species concentration. Moreover $\theta = T - T_\infty$ and $\phi = C - C_\infty$ are the differences of temperature and species concentration between fluid and ambient flow. Considered boundary conditions, under which (1) are solved, are as follows:

$$\begin{aligned} y = 0 : u(x,y,t) = v(x,y,t) = 0, \\ -\kappa \frac{\partial T}{\partial y} = q_w(x)\left[1 + \varepsilon \exp(i\omega t)\right], \\ -D\frac{\partial C}{\partial y} = c_w(x)\left[1 + \varepsilon \exp(i\omega t)\right] \\ y \longrightarrow \infty : u(x,\infty,t) = v(x,\infty,t) = 0. \end{aligned} \tag{2}$$

This set of boundary conditions suggests the form of the solutions of (1) as

$$\begin{aligned} u &= u_0(x,y) + \varepsilon \exp(i\omega t)\, u_1(x,y), \\ v &= v_0(x,y) + \varepsilon \exp(i\omega t)\, v_1(x,y), \\ T - T_\infty &= \left(\theta_0(x,y) + \varepsilon \exp(i\omega t)\, \theta_1(x,y)\right), \\ C - C_\infty &= \left(\phi_0(x,y) + \varepsilon \exp(i\omega t)\, \phi_1(x,y)\right), \end{aligned} \tag{3}$$

where ω represents the frequency of oscillation and ε, which is very very small positive number, measures the amplitude. Considering these forms of solutions, the steady mean flow is governed by the following set of equations:

$$\frac{\partial u_0}{\partial x} + \frac{\partial v_0}{\partial y} = 0, \tag{4}$$

$$u_0\frac{\partial u_0}{\partial x} + v_0\frac{\partial u_0}{\partial y} = \nu\frac{\partial^2 u_0}{\partial y^2} + g\beta_T\theta_0 + g\beta_C\phi_0, \tag{5}$$

$$u_0\frac{\partial \theta_0}{\partial x} + v_0\frac{\partial \theta_0}{\partial y} = \alpha\frac{\partial^2 \theta_0}{\partial y^2}, \tag{6}$$

$$u_0\frac{\partial \phi_0}{\partial x} + v_0\frac{\partial \phi_0}{\partial y} = D\frac{\partial^2 \phi_0}{\partial y^2} \tag{7}$$

subject to the boundary conditions:

$$\begin{aligned} y = 0 : \\ u_0 = v_0 = 0, \\ \theta_0' = -q_w(x), \\ \phi_0' = -c_w(x), \\ y \longrightarrow \infty : \\ u_0 \longrightarrow 0, \\ \theta_0 \longrightarrow 0, \\ \phi_0 \longrightarrow 0. \end{aligned} \tag{8}$$

The unsteady flow field is governed by the set of following differential equations and corresponding boundary conditions (9):

$$\begin{aligned} &\frac{\partial u_1}{\partial x} + \frac{\partial v_1}{\partial y} = 0, \\ &u_0\frac{\partial u_1}{\partial x} + u_1\frac{\partial u_0}{\partial x} + v_0\frac{\partial u_1}{\partial y} + v_1\frac{\partial u_0}{\partial y} + i\omega\theta_1 + i\omega\phi_1 \\ &\quad = \alpha\frac{\partial^2 u_1}{\partial y^2} + g\beta_T\theta_1 + g\beta_C\phi_1, \\ &u_0\frac{\partial \theta_1}{\partial x} + u_1\frac{\partial \theta_0}{\partial x} + v_0\frac{\partial \theta_1}{\partial y} + v_1\frac{\partial \theta_0}{\partial y} + i\omega\theta_1 = \alpha\frac{\partial^2 \theta_1}{\partial y^2}, \\ &u_0\frac{\partial \phi_1}{\partial x} + u_1\frac{\partial \phi_0}{\partial x} + v_0\frac{\partial \phi_1}{\partial y} + v_1\frac{\partial \phi_0}{\partial y} + i\omega\phi_1 = D\frac{\partial^2 \phi_1}{\partial y^2}, \\ &y = 0 : \\ &u_1 = v_1 = 0, \\ &\theta_1' = -q_w(x), \\ &\phi_1' = -c_w(x), \\ &y \longrightarrow \infty : \\ &u_1 \longrightarrow 0, \\ &\theta_1 \longrightarrow 0, \\ &\phi_1 \longrightarrow 0. \end{aligned} \tag{9}$$

To get the similarity equations the following transformations are commenced:

$$\begin{aligned} \psi_0 &= C_2 x^{4/5} F(\eta), \\ \Theta(\eta) &= \frac{C_1\theta_0}{x^{1/5}(q_w/\kappa)}, \\ \Phi(\eta) &= \frac{C_1\phi_0}{x^{1/5}(c_w/D)}, \\ \eta &= \frac{C_1 y}{x^{1/5}}, \\ q_w(x) &= q_0 x^n, \\ c_w(x) &= c_0 x^n, \end{aligned} \tag{10}$$

where

$$\begin{aligned} q_w(x) &= q_0 x^n, \\ q_w(x) &= c_0 x^n \\ C_1 &= \left(\frac{g\beta q_w}{\kappa\nu^2}\right)^{1/5}, \end{aligned}$$

$$C_2 = \left(\frac{g\beta q_w \nu^3}{\nu^2 D} \right)^{1/5},$$
$$\beta = \beta_T + \beta_C, \tag{11}$$

where ψ_0 is the stream function which satisfies the continuity equation (4) and q_0 and c_0 are the constants related to mean surface heat flux and mass flux, respectively. By introducing the above-mentioned set of transformations, the following sets of equations along with the boundary conditions are found for the steady flow:

$$\begin{aligned}
&F''' + \frac{n+4}{5} FF'' - \frac{2n+3}{5} \left(F'\right)^2 + (1-w)\,\Theta + w\Phi \\
&\quad = 0, \\
&\frac{1}{\mathrm{Pr}} \Theta'' + \frac{n+4}{5} F\Theta' - \frac{4n+1}{5} F'\Theta = 0, \\
&\frac{1}{\mathrm{Sc}} \Phi'' + \frac{n+4}{5} F\Phi' - \frac{4n+1}{5} F'\Phi = 0, \\
&F(0) = F'(0) = 0, \\
&\Theta'(0) = \Phi'(0) = -1, \\
&F'(\infty) = \Theta(\infty) = \Phi(\infty) = 0
\end{aligned} \tag{12}$$

and the transformations for the nonsimilarity equations are as follows:

$$\begin{aligned}
&\Psi_1 = C_2 x^{4/5} f(\eta, \xi), \\
&\theta(\eta) = \frac{C_1 \theta_1}{x^{1/5} q_w / \kappa}, \\
&\phi(\eta) = \frac{C_1 \phi_1}{x^{1/5} c_w / D}, \\
&\eta = \frac{C_1 y}{x^{1/5}}, \ \xi = \omega \left(\frac{\kappa x}{g\beta q_w \nu} \right)^{2/5}.
\end{aligned} \tag{13}$$

Equations for the unsteady flow field are as follows:

$$f''' + \frac{n+4}{5} Ff'' - \left(i\xi + \frac{4n+6}{5} F' \right) f' + \frac{n+4}{5} F'' f + (1-w)\,\theta + w\phi = \frac{2(1-n)}{5} \xi \left(F' \frac{\partial f'}{\delta \xi} - F'' \frac{\partial f}{\partial \xi} \right), \tag{14}$$

$$\frac{1}{\mathrm{Pr}} \theta'' + \frac{n+4}{5} F\theta' - \left(i\xi + \frac{4n+1}{5} F' \right) \theta + \frac{n+4}{5} \Theta' f - \frac{4n+1}{5} \Theta f' = \frac{2(1-n)}{5} \xi \left(F' \frac{\partial \theta}{\partial \xi} - \Theta' \frac{\partial f}{\partial \xi} \right), \tag{15}$$

$$\frac{1}{\mathrm{Sc}} \phi'' + \frac{n+4}{5} F\phi' - \left(i\xi + \frac{4n+1}{5} F' \right) \Phi + \frac{n+4}{5} \Phi' f - \frac{4n+1}{5} \Phi f' = \frac{2(1-n)}{5} \xi \left(F' \frac{\partial \phi}{\partial \xi} - \Phi' \frac{\partial f}{\partial \xi} \right). \tag{16}$$

Corresponding boundary conditions are

$$\begin{aligned}
&f(\xi, 0) = f'(\xi, 0) = 0, \\
&\theta'(\xi, 0) = \phi'(\xi, 0) = -1, \\
&f'(\xi, \infty) = \theta(\xi, \infty) = \phi(\xi, \infty) = 0.
\end{aligned} \tag{17}$$

Unsteady shear stress, surface temperature, and surface concentration are the most important quantities which should be taken into account to understand the flow field clearly and to elucidate the effects of corresponding important parameters on the flow pattern. These quantities can be calculated from the solutions of (11), (12), and (13)–(17). In this present study, these quantities are calculated and presented in terms of amplitude and phase angels. The following expressions are used to calculate the amplitude and phase of regarding quantities:

$$\begin{aligned}
&A_u = \sqrt{\left(f_r''\right)^2 + \left(f_i''\right)^2}\Big|_{\eta=0}, \\
&A_t = \sqrt{\left(\theta_r^2\right) + \left(\theta_i^2\right)}\Big|_{\eta=0}, \\
&A_c = \sqrt{\left(\phi_r^2\right) + \left(\phi_i^2\right)}\Big|_{\eta=0}, \\
&\phi_u = \tan^{-1}\left(\frac{f_i''}{f_r''} \right), \\
&\phi_t = \tan^{-1}\left(\frac{\theta_i}{\theta_r} \right), \\
&\phi_c = \tan^{-1}\left(\frac{\phi_i}{\phi_r} \right),
\end{aligned} \tag{18}$$

where $(f_r, f_i), (\theta_r, \theta_i)$, and (ϕ_r, ϕ_i) represent the real and imaginary part of $f(\xi, \eta), \theta(\xi, \eta)$, and $\phi(\xi, \eta)$, respectively. The solution methodologies for different parts of the flow field are discussed in brief in the following sections.

3. Solutions Methodologies

Three different techniques are used to solve the governing equations of the flow field. The implicit finite difference method of Keller [24] is put into operation for the entire regime, extended series solution (ESS) for small ξ which corresponds to the region near the leading edge, and asymptotic solution (ASS) for large ξ, corresponding to the region far from the leading edge. Comparisons amongst the results simulated by these three different techniques are elucidated in tabular form as well as by graphs. Excellent agreement amongst the simulated results by different numerical techniques ensured the validity of the model assumptions and efficiency of the numerical techniques that are applied here.

3.1. Extended Series Solutions (ESS). The results considering finite number of terms are valid only for very small range of frequencies. Since small values of ξ correspond to small

frequencies ω also, it can be predicted that the flow would be adjusted quasi-statically to the fluctuating rate of both heat and mass transfer in the boundary layer. For small values of ξ which corresponds to near the leading edge, the functions f, g, and h are expanded in power of ξ as given below:

$$f(\xi,\eta) = \sum_{n=0} (2i\xi)^m f_m(\eta),$$
$$g(\xi,\eta) = \sum_{n=0} (2i\xi)^m g_m(\eta), \tag{19}$$
$$h(\xi,\eta) = \sum_{n=0} (2i\xi)^m h_m(\eta).$$

Introducing the above-mentioned series in (13)–(16) and equating the terms of similar powers of ξ to zero, the following sets of equations can be obtained:

$$f_0''' + \frac{(n+4)}{5} F f_0'' - \frac{(4n+6)}{5} F' f_0' + \frac{(n+4)}{5} F'' f_0 + (1-w)\theta_0 + w\phi_0 = 0,$$
$$\frac{1}{\Pr}\theta_0'' + \frac{(n+4)}{5} F\theta_0' - \frac{(4n+1)}{5}\theta_0 F' - \frac{4n+1}{5}\Theta f_0' + \frac{n+4}{5}\Theta' f_0 = 0,$$
$$\frac{1}{\mathrm{Sc}}\phi_0'' + \frac{(n+4)}{5} F\phi_0' - \frac{(4n+1)}{5}\phi_0 F' - \frac{4n+1}{5}\Phi f_0' + \frac{n+4}{5}\Phi' f_0 = 0,$$
$$f_m''' + \frac{n+4}{5} F f_m'' + \left(\frac{2m(n-1)}{5} - \frac{4n+6}{5}\right) F' f_m' + \left(\frac{n+4}{5} - \frac{2m(n-1)}{5}\right) F'' f_m + \theta_m = \frac{1}{2} f_{m-1}', \tag{20}$$
$$\frac{1}{\Pr}\theta_m'' + \frac{n+4}{5} F\theta_m' + \left(\frac{2m(n-1)}{5} - \frac{4n+1}{5}\right) F'\theta_m - \frac{4n+1}{5}\Theta f_m' + \left(\frac{n+4}{5} - \frac{2m(n-1)}{5}\right)\theta' f_m = \frac{1}{2}\theta_{m-1},$$
$$\frac{1}{\mathrm{Sc}}\phi_m'' + \frac{n+4}{5} F\phi_m' + \left(\frac{2m(n-1)}{5} - \frac{4n+1}{5}\right) F'\phi_m - \frac{4n+1}{5}\Phi f_m' + \left(\frac{n+4}{5} - \frac{2m(n-1)}{5}\right)\varphi' f_m = \frac{1}{2}\phi_{m-1},$$

where $m = 1, 2, 3, \ldots$ and the respective boundary conditions are

$$f_0(0) = f_0'(0) = 0,$$
$$\theta_0'(0) = -1,$$
$$f_0'(\infty) = \theta_0(\infty) = 0,$$
$$f_m(0) = f_m'(0) = \theta_m(0) = 0,$$
$$f_m'(\infty) = \theta_m(\infty) = 0, \tag{21}$$

where primes denote the derivatives with respect to η as convention. In the above, f_0, g_0, and h_0 are the well-known free convection similarity solutions for steady flow field and the functions f_m, g_m, and h_m are the higher order corrections to the flow due to the effect of the transpiration of fluid through the surface of the plate. Moreover it can be observed that the equations are linear but coupled. Thus it can be assumed that the solutions can be calculated by pairwise sequential solution. Here, pair of equations are integrated using implicit Runge-Kutta-Butcher [25] initial value solver together with Nachtsheim and Swigert [26] iteration scheme. In this investigation, 8 pairs of equations are considered and solved numerically. Simulated results are compared with the results that are obtained by finite difference method and nice agreement was found amongst these three types of results.

3.2. Asymptotic Solution for Large ξ. To study the flow pattern far from the leading edge, that is, when the values of ξ are large, the asymptotic solutions are carried out. From the results obtained by Keller-Box method it is shown that for larger values of ξ the unsteady response is confined to a thin layer adjacent to the surface. Thus as frequency approaches towards infinity, the solutions tend to be independent of the distance measured downstream from the leading edge, similar to the shear wave solution in the corresponding forced flow problem. This suggested once again another set of series expansion utilizing the limiting solutions as the zeroth-order approximation:

$$Y = \xi^{1/2}\eta,$$
$$\varphi(\xi, Y) = \xi^{3/2} f(\xi,\eta),$$
$$\theta(\xi, Y) = \theta(\xi,\eta), \tag{22}$$
$$\phi(\xi, Y) = \phi(\xi,\eta).$$

Introducing these transformations, (14)–(16) take the form

$$\frac{\partial^3\varphi}{\partial Y^3} + \frac{n+4}{5} F\xi^{-1/2}\frac{\partial^2\varphi}{\partial Y^2} - i\frac{\partial\varphi}{\partial Y} - \frac{6n+4}{5} F'\xi^{-1}\frac{\partial\varphi}{\partial Y} + \frac{4n+1}{5} F''\xi^{-3/2}\varphi + (1-w)\theta + w\phi = \frac{2(1-n)}{5}\left[F'\left(\frac{\partial^2\varphi}{\partial Y\partial\xi} + \frac{Y}{2\xi}\frac{\partial^2\varphi}{\partial Y^2}\right) - F''\xi^{-1/2}\left(\frac{\partial\varphi}{\partial\xi} + \frac{Y}{2\xi}\frac{\partial\varphi}{\partial Y}\right)\right], \tag{23}$$

$$\frac{1}{\mathrm{Pr}}\frac{\partial^2\theta}{\partial Y^2}+\frac{n+4}{5}F\xi^{-1/2}\frac{\partial\theta}{\partial Y}-i\theta-\frac{4n+1}{5}F'\xi^{-1}\theta$$
$$-\frac{4n+1}{5}\Theta\xi^{-2}\frac{\partial\varphi}{\partial Y}+\frac{4n+1}{5}\Theta'\xi^{-5/2}\varphi$$
$$=\frac{2(1-n)}{5}\left[F'\left(\frac{\partial\theta}{\partial\xi}+\frac{Y}{2\xi}\frac{\partial\theta}{\partial Y}\right)\right.$$
$$\left.-\Theta'\xi^{-3/2}\left(\frac{\partial\varphi}{\partial\xi}+\frac{Y}{2\xi}\frac{\partial\varphi}{\partial Y}\right)\right], \tag{24}$$

$$\frac{1}{\mathrm{Sc}}\frac{\partial^2\phi}{\partial Y^2}+\frac{n+4}{5}F\xi^{-1/2}\frac{\partial\phi}{\partial Y}-i\phi-\frac{4n+1}{5}F'\xi^{-1}\phi$$
$$-\frac{4n+1}{5}\Phi\xi^{-2}\frac{\partial\varphi}{\partial Y}+\frac{4n+1}{5}\phi'\xi^{-5/2}\varphi$$
$$=\frac{2(1-n)}{5}\left[F'\left(\frac{\partial\phi}{\partial\xi}+\frac{Y}{2\xi}\frac{\partial\phi}{\partial Y}\right)\right.$$
$$\left.-\Phi'\xi^{-3/2}\left(\frac{\partial\varphi}{\partial\xi}+\frac{Y}{2\xi}\frac{\partial\varphi}{\partial Y}\right)\right], \tag{25}$$

respectively. We can express the functions F, Θ, and Φ with fine accuracy as power series. This is because the above equations represent the region which is confined to a thin layer adjacent to the surface. Here, the following series representations are used:

$$F=a_2\eta^2+\cdots, \tag{26}$$

$$\Theta=b-\eta+\cdots, \tag{27}$$

$$\Phi=c-\eta+\cdots, \tag{28}$$

where

$$a_2=\frac{1}{2}F''(0),$$
$$b=\Theta(0)=-1, \tag{29}$$
$$c=\Phi(0)=-1.$$

Implementing those above expansions, solutions of (14)–(16) can be found in the form of

$$\varphi(\xi,Y)=\sum_{n=0}\xi^{-m/2}\overline{f}_m(Y),$$
$$\theta(\xi,Y)=\sum_{n=0}\xi^{-m/2}\overline{\theta}_m(Y), \tag{30}$$
$$\phi(\xi,Y)=\sum_{n=0}\xi^{-m/2}\overline{\phi}_m(Y).$$

After substituting (33) into (14)–(16) and collecting similar powers of ξ, the following equations can be obtained:

$$\overline{f}_0'''-i\overline{f}_0'=-(1-w)\overline{\theta}_0-w\overline{\phi}_0, \tag{31}$$

$$\overline{f}_1'''-i\overline{f}_1'=-(1-w)\overline{\theta}_1-w\overline{\phi}_1, \tag{32}$$

$$\overline{f}_2'''-i\overline{f}_2'=-(1-w)\overline{\theta}_2-w\overline{\phi}_2, \tag{33}$$

$$\overline{f}_3'''-i\overline{f}_3'=-\frac{3n+2}{5}a_2Y^2\overline{f}_0''+\frac{2(7n+3)}{5}a_2Y\overline{f}_0'$$
$$-\frac{2(4n+1)}{5}a_2\overline{f}_0-(1-w)\overline{\theta}_3 \tag{34}$$
$$-w\overline{\phi}_3,$$

$$\frac{1}{\mathrm{Pr}}\overline{\theta}_0''-i\overline{\theta}_0=0, \tag{35}$$

$$\frac{1}{\mathrm{Pr}}\overline{\theta}_1''-i\overline{\theta}_1=0, \tag{36}$$

$$\frac{1}{\mathrm{Pr}}\overline{\theta}_2''-i\overline{\theta}_2=0, \tag{37}$$

$$\frac{1}{\mathrm{Pr}}\overline{\theta}_3''-i\overline{\theta}_3=-\frac{3n+2}{5}a_2Y^2\overline{\Theta}_0'+\frac{8n+2}{5}a_2Y\overline{\Theta}_0, \tag{38}$$

$$\frac{1}{\mathrm{Sc}}\overline{\phi}_0''-i\overline{\phi}_0=0, \tag{39}$$

$$\frac{1}{\mathrm{Sc}}\overline{\phi}_1''-i\overline{\phi}_1=0, \tag{40}$$

$$\frac{1}{\mathrm{Sc}}\overline{\phi}_2''-i\overline{\phi}_2=0, \tag{41}$$

$$\frac{1}{\mathrm{Sc}}\overline{\phi}_3''-i\overline{\phi}_3=-\frac{3n+2}{5}a_2Y^2\overline{\Phi}_0'+\frac{8n+2}{5}a_2Y\overline{\Phi}_0. \tag{42}$$

In these equations, primes denote the differentiation with respect to Y, and the associated boundary conditions are

$$\overline{f}_m(0)=\overline{f}_m'(0)=\overline{f}_m'(\infty)=0,\quad m=0,1,2,3,4,\ldots,$$
$$\overline{\theta}_0'(0)=-1,$$
$$\overline{\theta}_m(0)=\overline{\theta}_m(\infty)=0,\quad m=0,1,2,3,4,\ldots, \tag{43}$$
$$\overline{\phi}_0'(0)=-1,$$
$$\overline{\phi}_m(0)=\overline{\phi}_m(\infty)=0,\quad m=0,1,2,3,4,\ldots.$$

The solutions of (31)–(42) subject to the boundary conditions (43) give the following expressions for shear stress, surface temperature, and species concentration, respectively:

$$f''(\xi,0)$$
$$=-i\left(\frac{an1}{\sqrt{\mathrm{Pr}}\left(1+\sqrt{\mathrm{Pr}}\right)}+\frac{an2}{\sqrt{\mathrm{Sc}}\left(1+\sqrt{\mathrm{Sc}}\right)}\right)\xi^{-1/2}$$
$$+2\left(C_{12}+C_{22}+C_{32}\right)$$

$$
\begin{aligned}
&- 2\sqrt{i}\left(C_{13} + \sqrt{\mathrm{Pr}}C_{23} + \sqrt{\mathrm{Sc}}C_{33}\right) + i\mathrm{Pr}C_{24} \\
&+ i\mathrm{Sc}C_{34}\xi^{-5/2} + O\left(\xi^{-7/2}\right), \\
\theta(\xi,0) &= \frac{1}{\sqrt{i\mathrm{Pr}}}\xi^{-1/2} + \frac{(11n+4)\,a_2}{20\mathrm{Pr}}\xi^{-5/2} + O\left(\xi^{-7/2}\right), \\
\phi(\xi,0) &= \frac{1}{\sqrt{i\mathrm{Sc}}}\xi^{-1/2} + \frac{(11n+4)\,a_2}{20\mathrm{Sc}}\xi^{-5/2} + O\left(\xi^{-7/2}\right),
\end{aligned} \tag{44}
$$

where

$$
\begin{aligned}
A &= \frac{(1-w)}{\mathrm{Pr}\,(1-\mathrm{Pr})}, \\
B &= \frac{w}{\mathrm{Sc}\,(1-\mathrm{Sc})}, \\
C_3 &= \frac{(1-w)\,\sqrt{\mathrm{Pr}}}{\mathrm{Pr}\,(1-\mathrm{Pr})} - \frac{w\sqrt{\mathrm{Sc}}}{\mathrm{Sc}\,(1-\mathrm{Sc})}, \\
A_1 &= -\frac{(3n+2)\,a_2\sqrt{\mathrm{Pr}}}{30\sqrt{i}}, \\
B_1 &= \frac{(11n+4)\,a_2 i}{20}, \\
C_1 &= \frac{(11n+4)\,a_2\sqrt{i}}{20\sqrt{\mathrm{Pr}}}, \\
A_2 &= -\frac{(3n+2)\,a_2\sqrt{\mathrm{Sc}}}{30\sqrt{i}}, \\
B_2 &= \frac{(11n+4)\,a_2 i}{20}, \\
C_2 &= \frac{(11n+4)\,a_2\sqrt{i}}{20\sqrt{\mathrm{Sc}}}, \\
P_1 &= -\frac{(3n+2)\,a_2}{5}, \\
P_2 &= -\frac{2\,(7n+3)\,a_2}{5}, \\
P_3 &= -\frac{2\,(4n+1)\,a_2}{5}, \\
C_{11} &= \frac{P_1 C_3}{6}, \\
C_{12} &= \frac{1}{4\sqrt{i}}P_2 C_3 + 18C_{11}, \\
C_{13} &= \frac{1}{2i}P_3 C_3 + 6\sqrt{i}C_{12} - 6C_{11}, \\
C_{21} &= -\frac{(1-w)\,(3n+2)\,a_2}{30\,(1-\mathrm{Pr})}, \\
C_{22} &= -\frac{(1-w)\,a_2 K_1}{20\sqrt{i\mathrm{Pr}}\,(1-\mathrm{Pr})^2}, \\
C_{23} &= -\frac{(1-w)\,a_2 K_2}{20i\mathrm{Pr}\,(1-\mathrm{Pr})^3}, \\
C_{31} &= -\frac{w\,(3n+2)\,a_2}{30\,(1-\mathrm{Sc})}, \\
C_{32} &= -\frac{w a_2 K_{11}}{20\sqrt{i\mathrm{Sc}}\,(1-\mathrm{Sc})^2}, \\
C_{33} &= -\frac{w a_2 K_{22}}{20i\mathrm{Sc}\,(1-\mathrm{Sc})^3}, \\
K_1 &= 4\,(3n+2) + (1-\mathrm{Pr})\,(11n+4) \\
&\quad + 2\,(3n+2)\,(1-3\mathrm{Pr}), \\
K_2 &= 8\,(1-\mathrm{Pr})\,(7n+3) + (11n+4)\,(1-\mathrm{Pr})^2 \\
&\quad + 4\,(1-3\mathrm{Pr})\,K_1 + 12\mathrm{Pr}\,(1-\mathrm{Pr})\,(3n+2), \\
K_{11} &= 4\,(3n+2) + (1-\mathrm{Sc})\,(11n+4) \\
&\quad + 2\,(3n+2)\,(1-3\mathrm{Sc}), \\
K_{22} &= 8\,(1-\mathrm{Sc})\,(7n+3) + (11n+4)\,(1-\mathrm{Sc})^2 \\
&\quad + 4\,(1-3\mathrm{Sc})\,K_1 + 12\mathrm{Sc}\,(1-\mathrm{Sc})\,(3n+2).
\end{aligned} \tag{45}
$$

The above expressions are valid only for $\mathrm{Pr} \neq 1$ and $\mathrm{Sc} \neq 1$. If it is necessary to calculate the values for $\mathrm{Pr} = 1$ and $\mathrm{Sc} = 1$ then the limiting values as $\mathrm{Pr} \to \infty$ and $\mathrm{Sc} \to \infty$ should be calculated.

4. Results and Discussions

Since natural convection flow due to combined effects of thermal and mass diffusion is very important in practical point of view, an extensive investigation for this type of model flow field has been carried out through numerical simulations. In view of the fact that Hossain et al. (1998) also examined this type of flow field only for thermal diffusion, in this present investigation, similar types of results, discussed by Hossain et al. (1998), are produced first. Then the model has been extended to study the flow field with both thermal and mass diffusion. All the model assumptions are kept similar to Hossain et al. (1998). Both the steady and fluctuating parts of the problem are analyzed by the Keller-Box method for the entire frequency regime. The fluctuating part of the problem is investigated by three different methodologies. Results are presented in amplitude and phase angles forms for variation of different parameters in both tabular and graphical forms. The forgoing formulations may be analyzed to indicate the nature of the interaction of the various contributions to buoyancy. These may aid or oppose one another and be of different magnitudes characterized by the value of w. When the thermal and solutal effects are opposed, the value of w is negative in order to ensure that the flow is in positive x

Table 1: Values of shear stress, surface temperature, and surface concentration for the steady flow field for variation of different parameters while Pr = 0.7.

	Shear stress	Surface temperature	Surface concentration
w			
0.0000	0.56578	0.33272	0.59525
0.2500	0.50978	0.31013	0.54862
0.7500	0.46897	0.29386	0.51562
1.000	0.41226	0.27140	0.47100
n			
0.0000	0.44347	0.38467	0.72034
0.2500	0.40040	0.35692	0.66014
0.7500	0.36891	0.33708	0.61773
1.000	0.32501	0.30994	0.56078
Sc			
0.1000	0.56920	0.26926	0.68102
0.6000	0.37955	0.33184	0.35711
1.1000	0.34202	0.35068	0.28454
1.6000	0.32396	0.35963	0.24756

direction. The relative physical extent η of the two effects in convection region is governed by the magnitudes of the Prandtl number and Schmidt number and their relative values. Here, discussions are restricted for favorable case only (w is positive) for the fluids with Prandtl number Pr = 0.9–0.25. Here, the values of Prandtl numbers are chosen to represent the fluid as air and liquid which are currently used as coolant in nuclear engineering. Although the diffusing chemical species of most common interest in air has Schmidt numbers in the range from 0.1 to 10.0, the present investigation considered a range from 0.1 to 1.60.

Some values of shear stress, surface temperature, and surface concentration for the steady flow field are listed in Table 1. During the simulations, the value of Prandtl number, Pr, is chosen as constant value 0.7, representing air, and all other parameters are varied. It can be observed from Table 1 that the values of shear stress, surface temperature, and surface concentration decrease as the values of w, n, and Sc become higher.

Tables 2 and 3 show the comparison of the results obtained by Keller-Box method and perturbation method for local surface temperature and local mass concentration, respectively. For these simulations, the values of the parameters w, n, Pr, and Sc are taken as 0.5, 0.5, 0.7, and 0.22, respectively, and the quantities represented against ξ ranging from 0.00 to 70.00. The required quantities for the small value of ξ (0.0–0.9) are obtained from extended series solution method and for the higher values of ξ (1.0–70.0) the respective quantities are taken from the results by asymptotic series solution method. For both amplitude and phase angels of the respective quantities, nice agreement is found amongst the results calculated by different methodologies. Here also plodding decrement of amplitude of shear stress, surface temperature and surface concentration, and increment of phase angels of the respective quantities along with the increment of the values of ξ can be observed.

Table 2: Comparison of the values of amplitude and phase angels of the local surface temperature, obtained by perturbation methods and finite difference method, while Pr = 0.7, Sc = 0.22, w = 0.5, and n = 0.5.

ξ	A_T		ϕ_T	
	Keller	Series and asymp.	Keller	Series and asymp.
0.0000	1.4273	1.42738[1]	0.00000	0.00000[1]
0.1002	1.42469	1.42627[1]	2.99340	2.68514[1]
0.2013	1.41650	1.42292[1]	5.99132	5.37870[1]
0.3045	1.40272	1.40877[1]	8.99521	7.08826[1]
0.4108	1.38327	1.38864[1]	12.00221	9.81945[1]
0.5024	1.36270	1.36990[1]	14.50581	8.39808[1]
0.5975	1.33815	1.33728[1]	17.00177	9.81636[1]
0.6967	1.30965	1.31337[1]	19.48248	11.24410[1]
0.8009	1.27723	1.29649[1]	21.93677	12.84996[1]
0.9105	1.24099	1.25415[1]	24.34766	14.08462[1]
1.0028	1.20936	1.23616[2]	26.22925	15.45600[2]
1.5095	1.03562	2.03802[2]	34.05537	19.7270[2]
1.6019	1.00658	1.88270[2]	35.04818	20.7739[2]
1.6984	0.97772	1.74540[2]	35.96272	21.8113[2]
1.7991	0.94923	1.6235[2]	36.79935	22.8364[2]
1.9043	0.92130	1.5149[2]	37.56064	23.8464[2]
2.0143	0.89404	1.4176[2]	38.25065	24.8384[2]
5.0216	0.54424	0.6023[2]	43.57451	37.9955[2]
6.0502	0.49349	0.5428[2]	43.94037	39.2737[2]
7.0417	0.45604	0.4520[2]	44.16434	40.3392[2]
8.0555	0.42544	0.4281[2]	44.32133	41.2201[2]
9.0596	0.40053	0.4219[2]	44.43331	42.7183[2]
10.0179	0.38044	0.3979[2]	44.51393	42.1542[2]
20.2113	0.26657	0.2708[2]	44.83141	43.9730[2]
30.1619	0.21795	0.2198[2]	44.90746	44.4320[2]
40.0461	0.18905	0.1885[2]	44.93943	44.6366[2]
50.5732	0.16818	0.1603[2]	44.95727	44.7304[2]
60.7511	0.15342	0.1539[2]	44.96755	44.8000[2]
70.5839	0.14232	0.1427[2]	44.97404	44.84020[2]

[1]Standing for series solution; [2]standing for asymptotic solution.

The effects of Prandtl number Pr and the exponent parameter n on the shear stress are presented in Figures 1 and 2. All the graphs for depicting the amplitudes and phase angels of shear stress are drawn for the results obtained from numerical simulations by Keller-Box method, extended series solution method, and asymptotic series solution method. All the figures clearly show that results obtained for the entire regime are significantly close to the results that are calculated for the region near and far from the leading edge.

For different values of Pr, while all other parameters are kept constant (w = 0.5, n = 0.5, and Sc = 0.6), remarkable increase can be seen in amplitudes of the shear stress due to the increment of the Prandtl number, Pr. The phase angels are zero under quasi-steady conditions and decrease monotonically towards the asymptotic values -90° as $\xi \to \infty$.

Table 3: Comparison of the values of amplitude and phase angels of the local surface concentration, obtained by perturbation method and finite difference method, while Pr = 0.7, Sc = 0.22, $w = 0.5$, and $n = 0.5$.

ξ	A_c		ϕ_c	
	Keller	Series and asymp.	Keller	Series and asymp.
0.0000	1.53621	1.53620[1]	0.00000	0.00000[1]
0.1002	1.53298	1.53484[1]	3.02864	3.42313[1]
0.2013	1.52326	1.53484[1]	6.04759	5.00983[1]
0.3045	1.50730	1.52422[1]	9.04992	5.13372[1]
0.4108	1.48535	1.51529[1]	12.03249	6.83417[1]
0.5024	1.46265	1.50561[1]	14.50248	8.33942[1]
0.5975	1.43599	1.49615[1]	16.95796	9.79256[1]
0.6967	1.40540	1.48654[1]	19.39603	10.85799[1]
0.8009	1.37088	1.47676[1]	21.80920	11.00362[1]
0.9105	1.33244	1.47121[1]	24.18315	12.87376[1]
1.0995	1.26326	1.46922[2]	27.84154	13.63863[2]
1.6984	1.05333	1.9636[2]	35.72082	20.8994[2]
1.7991	1.02297	1.8229[2]	36.56183	21.9220[2]
1.9043	0.99316	1.6977[2]	37.32884	22.9334[2]
2.0143	0.96403	1.5857[2]	38.02563	23.9307[2]
2.0904	0.94505	1.5857[2]	38.45352	24.9113[2]
2.2089	0.91727	1.3948[2]	39.04424	25.8726[2]
4.0219	0.66171	0.7996[2]	42.83438	34.6990[2]
5.0216	0.58795	0.6577[2]	43.48498	37.5134[2]
6.0502	0.53315	0.5914[2]	43.86996	38.8672[2]
7.0417	0.49270	0.5352[2]	44.10680	40.0001[2]
8.0555	0.45964	0.4867[2]	44.27340	40.9397[2]
9.0596	0.43272	0.4720[2]	44.39253	41.4722[2]
10.0179	0.41102	0.4315[2]	44.47848	41.9387[2]
20.2113	0.28796	0.2929[2]	44.81842	43.8923[2]
30.1619	0.23543	0.2376[2]	44.90023	44.3870[2]
40.0461	0.20421	0.2037[2]	44.93467	44.6077[2]
50.5732	0.18167	0.1840[2]	44.95390	44.7089[2]
60.7511	0.16572	0.1663[2]	44.96498	44.7840[2]
70.5839	0.15373	0.1541[2]	44.97199	44.8274[2]

[1]Standing for series solution; [2]standing for asymptotic solution.

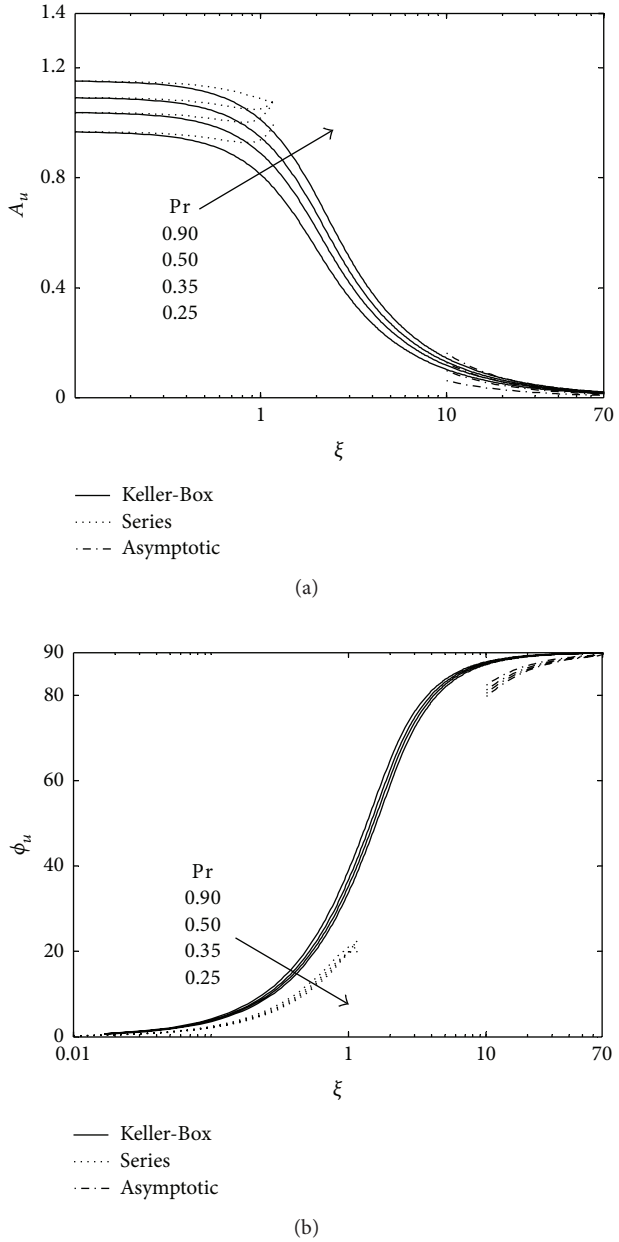

Figure 1: (a) Amplitude and (b) phase angles, of shear stress for different values of Pr, while Sc = 0.6, $w = 0.5$, and $n = 0.5$.

From Figure 2, it can be observed that the amplitudes of the shear stress are decreased while the exponents of the surface heat and mass flux are increased. But the values of phase angels of shear stress are increased as the values of exponent increase. For much higher values of ξ, that is, far from the leading edge, there is almost no change in values of amplitude for variation of n and the corresponding values tend to zero for all values of n.

The effects of Prandtl number, Pr, on the amplitudes and phase angels of the surface temperature are illustrated in Figure 3. For these simulations, the values of w and n are taken as 0.5 and the value of Sc is chosen as 0.6. In these figures also, results are presented for three different methodologies, as described in the previous sections. For the very low frequency region, that is, for the very small values of ξ, the results obtained by extended series solution method are very much close to the solutions that are obtained from Keller-Box method. Far from the leading edge, that is, for the large values of ξ, we can see very nice agreement between the results obtained from the asymptotic solutions and Keller-Box solutions. It can also be seen from these figures that the values of amplitudes of surface temperature decrease as the values of Pr increase. The values of phase angels for surface temperature increase for the decrement of the values of Pr. The values of phase angles tend towards the value of -45° as the value of $\xi \to \infty$.

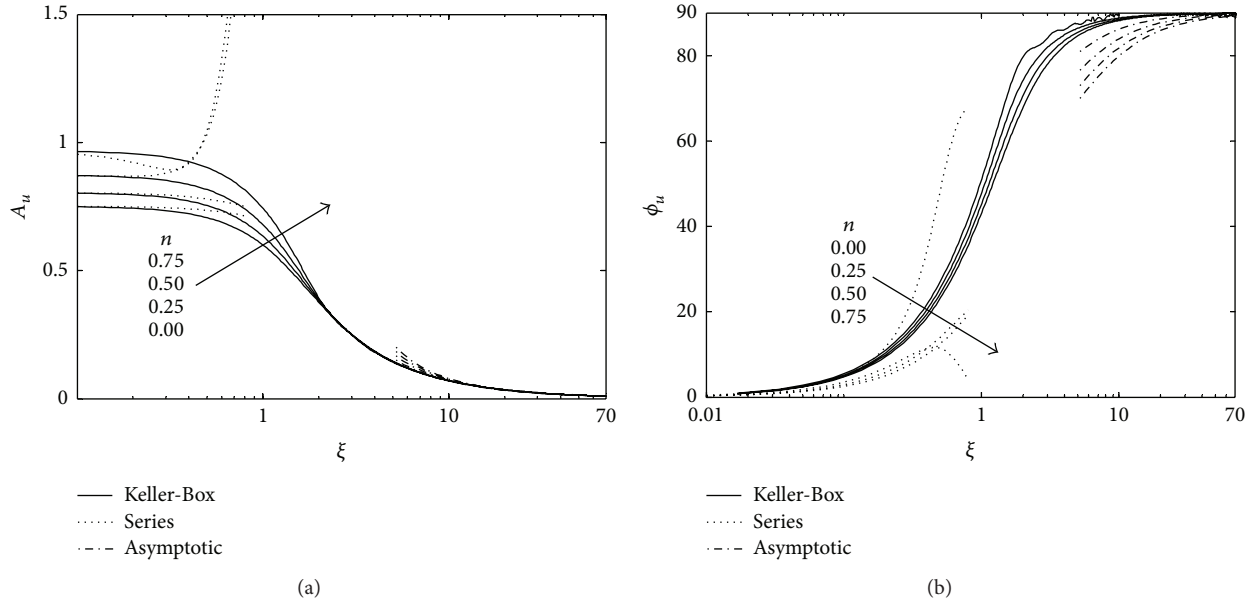

Figure 2: (a) Amplitude and (b) phase angels, of shear stress for different values of n, while Pr = 0.7, Sc = 0.6, and $w = 0.5$.

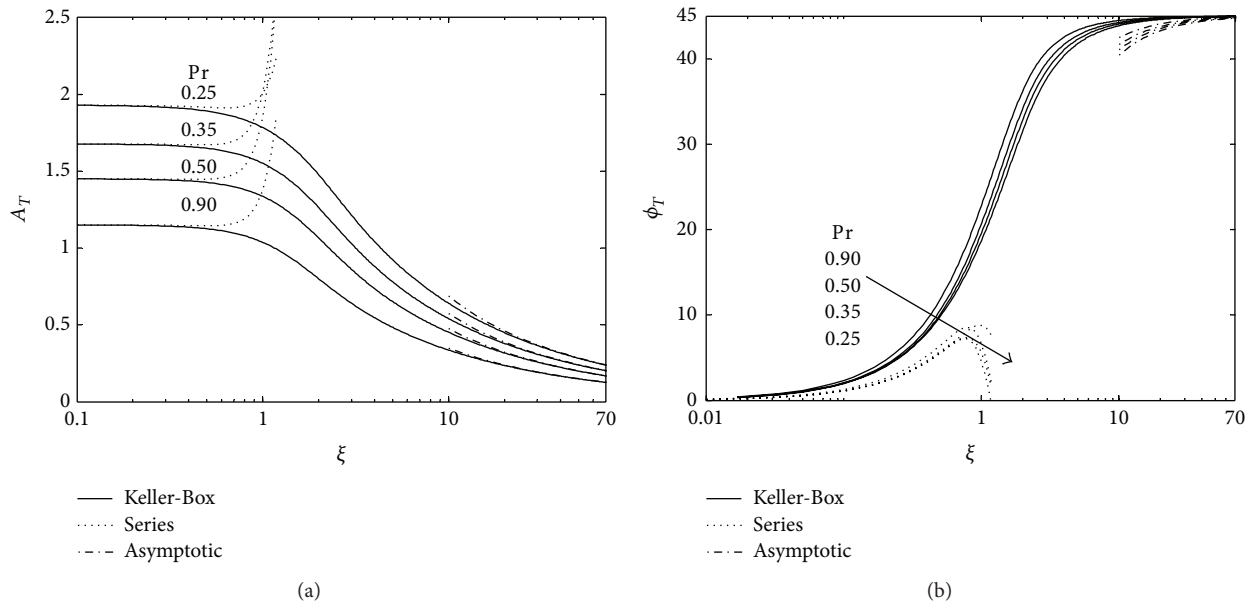

Figure 3: (a) Amplitude and (b) phase angles, of surface temperature for different values of Pr, while Sc = 0.6, $w = 0.5$, and $n = 0.5$.

In Figure 4, the effect of exponent parameter n on the surface temperature is presented. Similar to shear stress, here also the values of amplitude of surface temperature become little smaller as the values of n become higher and far from the leading edge; that is, for the large values of ξ, these changes become ignorable for the variation of n and tend toward the value of zero. For the phase angels, as expected, the opposite behavior is observed; that is, very small increment of the quantities is achieved because of small decrement of values of n.

Similar types of behavior can be observed for the surface mass concentration for different values of Schmidt number, Sc, in Figure 5. During the simulation, to predict the effects of Schmidt numbers on both the surface mass concentration and shear stress, the value of Prandtl number is taken as 0.7 and the values of w and n are chosen as 0.5. We can monitor the increment of the values of amplitude of surface species concentration as the values of Sc are decreased while the values of phase angels increased in small amount. As the values of ξ get higher, the value of the phase angles of

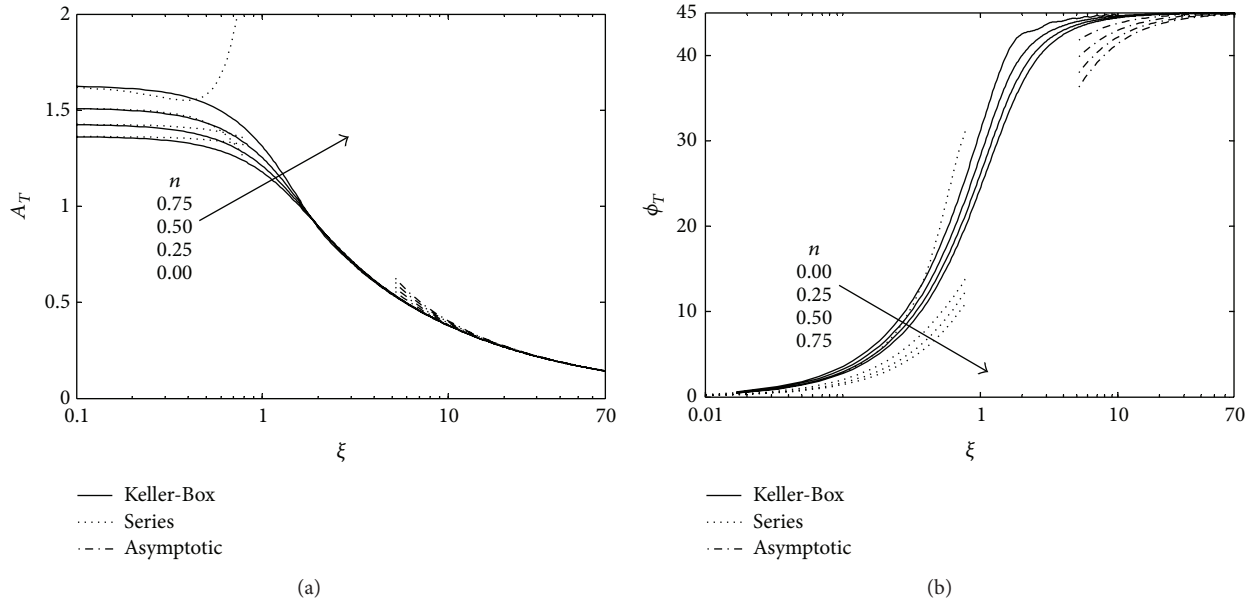

Figure 4: (a) Amplitude and (b) phase angles of surface temperature for different values of n, while Pr = 0.7, Sc = 0.6, and $w = 0.5$.

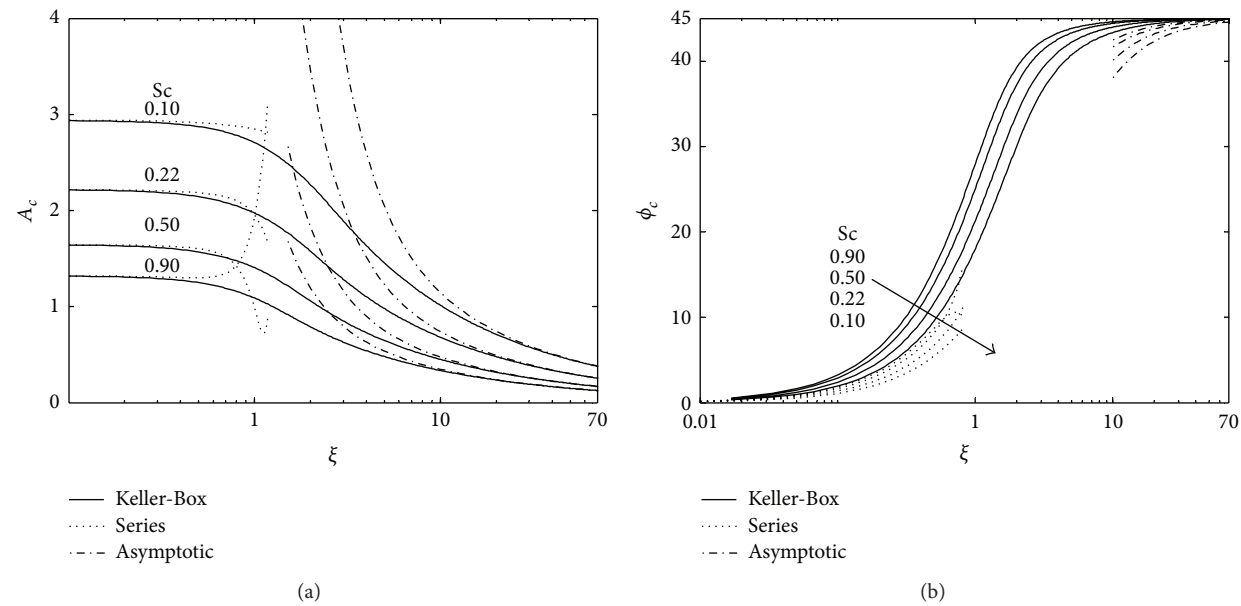

Figure 5: (a) Amplitude and (b) phase angles of surface concentration for different values of Sc, while Pr = 0.7, $w = 0.5$, and $n = 0.5$.

the surface mass concentration reached the asymptotic value of -45°.

4.1. Effects of Different Parameters on Transient Shear Stress, Transient Surface Temperature, and Transient Surface Concentration. In this section, the effects of some parameters such as Schmidt number Sc, amplitude of thermal and mass flux ε, buoyancy ratio parameter w, and the flux exponent parameter n on the transient shear stress, transient surface temperature, and transient surface concentration are discussed at $\xi = 1.00$. All these results are presented here for a fixed Prandtl number, Pr, which is taken once again as 0.70. The definitions for transient shear stress, τ, transient surface temperature, θ_w, and transient surface concentration, ϕ_w, have been used as follows:

$$\begin{aligned} \tau &= \tau_s + \varepsilon A_u \cos\left(\omega t + \phi_u\right), \\ \theta_w &= \theta_s + \varepsilon A_t \cos\left(\omega t + \phi_t\right), \\ \phi_w &= \phi_s + \varepsilon A_c \cos\left(\omega t + \phi_c\right), \end{aligned} \tag{46}$$

where τ_s is the steady mean shear stress, θ_s is the steady surface temperature, and ϕ_s is the steady surface concentration, respectively. The values of τ_s, θ_s, and ϕ_s are calculated first and

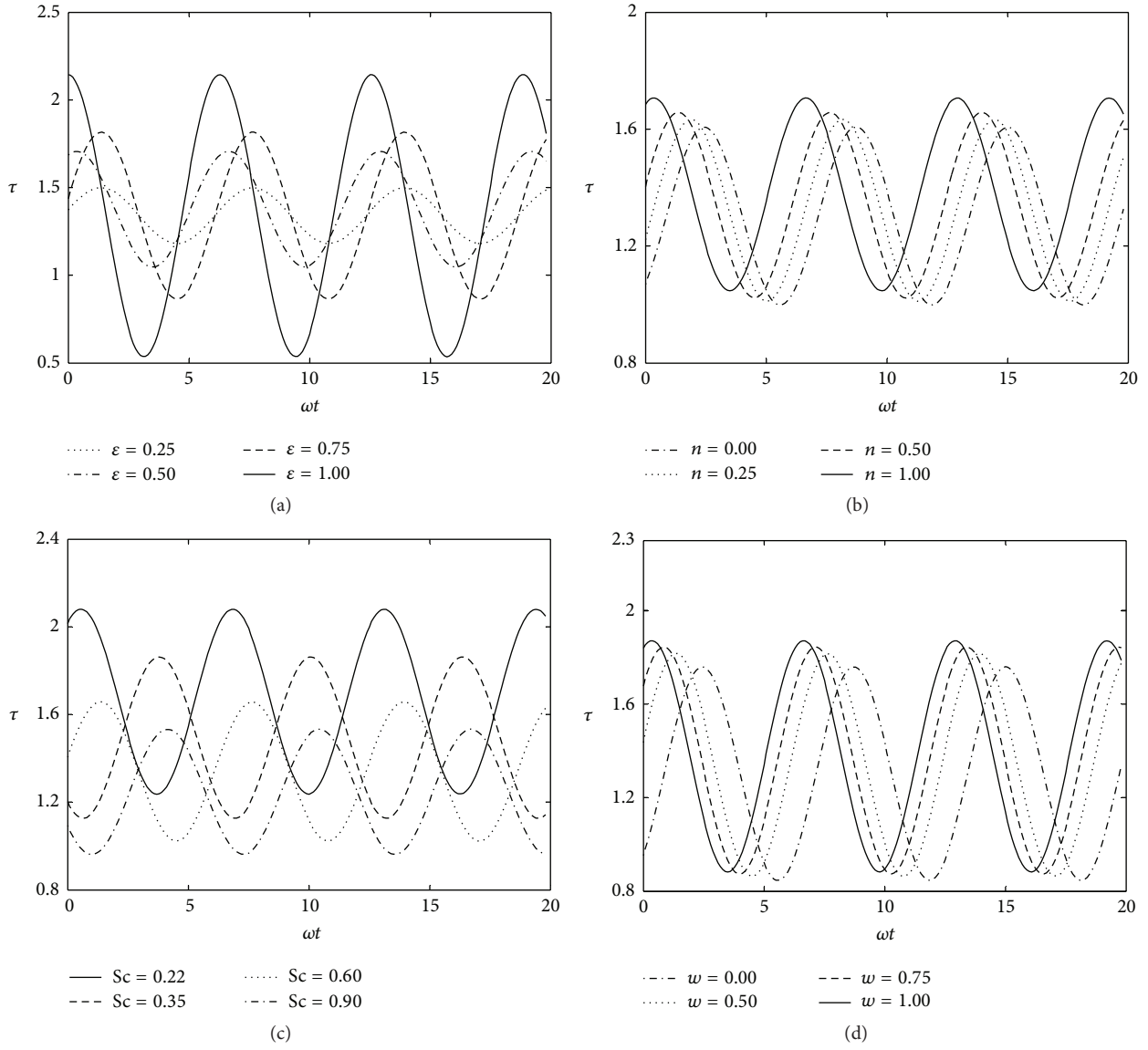

FIGURE 6: Transient shear stress at $\xi = 1.0$ for different (a) ε, while Pr = 0.7, Sc = 0.6, $w = 0.5$, and $n = 0.5$, (b) n, while Pr = 0.7, Sc = 0.6, and $w = 0.0$, (c) Sc, while Pr = 0.7, $w = 0.5$, and $n = 0.5$, and (d) w, while Pr = 0.7, $n = 0.5$, and Sc = 0.6.

then the required quantities are obtained accordingly from the simulations by using the implicit finite difference method together with the Keller-Box for the entire regime.

From Figures 6(a), 7(a), and 8(a), it can be seen that the increase in the values of amplitude of oscillation of surface temperature and surface concentration caused increment in the oscillation of transient skin friction, transient surface temperature, and transient surface concentration, respectively. The oscillations with different values of amplitude and phase with regular periodic maxima and minima are visualized in Figures 6(b), 7(b), and 8(b) for the heat and mass flux exponent parameter n. The oscillations patterns of the transient skin friction, surface temperature, and surface concentration are similar. From Figures 6(c), 7(c), and 8(c), it can be seen that the oscillations of the amplitude of transient shear stress, transient surface temperature, and transient surface concentration decrease as the values of Sc increase. For each value of Sc, these oscillations attain a maximum and a minimum value periodically. For buoyancy ratio parameter w, a periodic oscillation for transient skin friction, transient surface temperature, and transient surface concentration is shown. For the variation of the values of w, no significant changes occurred for the corresponding maximum and minimum values of the oscillations.

5. Conclusion

The purpose of this study is to investigate the velocity flow field in terms of local shear stress. Local heat and mass transfer resulting from buoyancy forces which arise from a combination of temperature and species concentration effects of comparable magnitude are also studied rigorously.

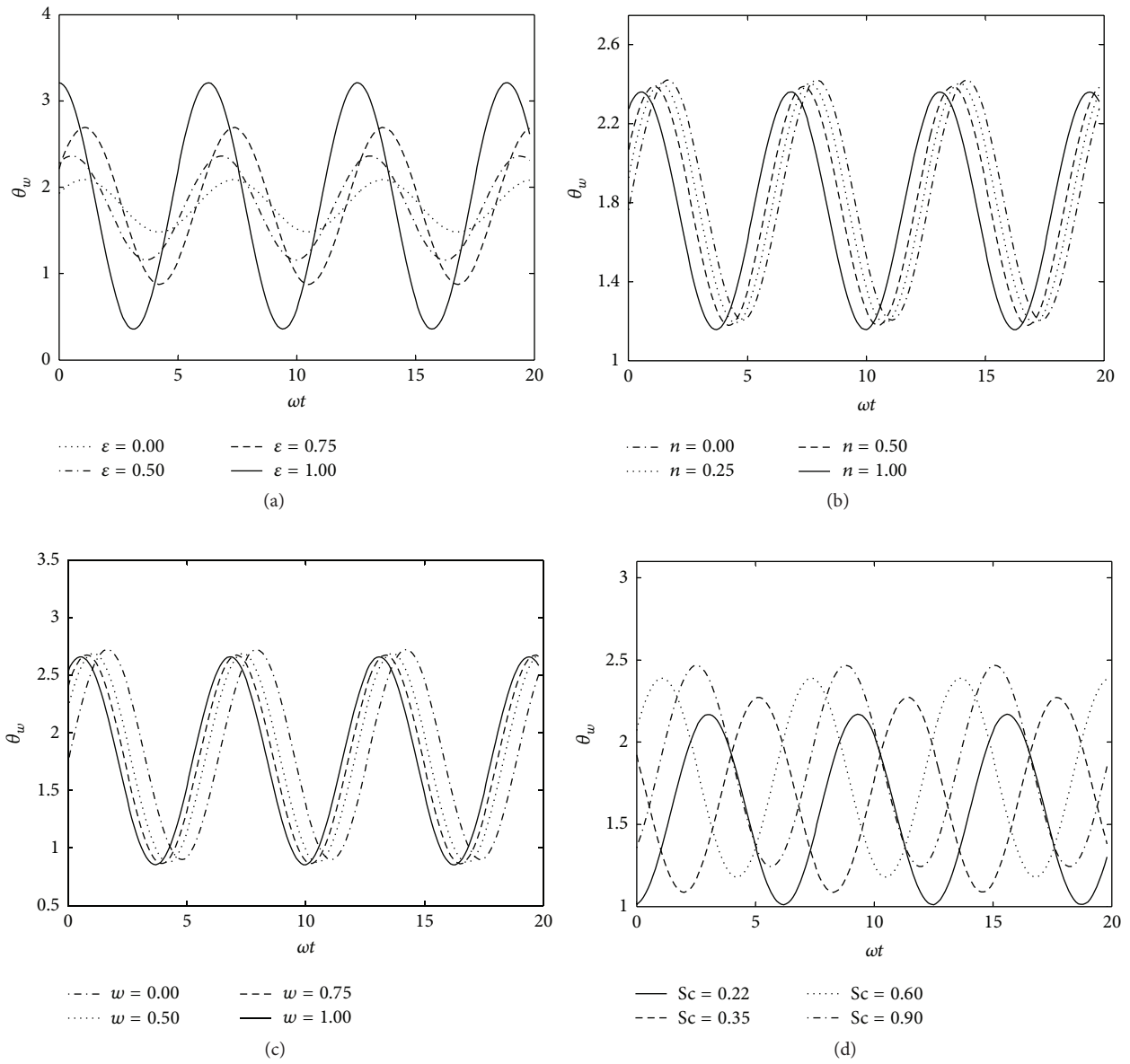

Figure 7: Transient surface temperature at $\xi = 1.0$ for different (a) ε, while Pr = 0.7, Sc = 0.6, $w = 0.5$, and $n = 0.5$, (b) n, while Pr = 0.7, Sc = 0.6, and $w = 0.0$, (c) w, while Pr = 0.7, Sc = 0.6, and $n = 0.5$, and (d) w, while Pr = 0.7, $n = 0.5$, and Sc = 0.6.

A linearized theory has been utilized and detailed numerical calculations are carried out for wide ranges of parameters. The important findings of this study can be summarised as follows.

(i) Exceptive agreement amongst all the results calculated by different numerical methods established the validity of the simulations as well as the assumptions of the mathematical model that are made for the respective flow field.

(ii) From the analysis of hydrodynamics heat and mass transfer, a complex correlation can be observed among the flow pattern, wall shear stress, and mass transfer enhancement along the flow channel being dependent on the different parameters.

(iii) From the observations of the simulated results it can be concluded that the amplitude of the shear stress, local heat transfer, and local mass transfer decreased as the frequency increases despite the consequences of the Prandtl number, Schmidt number, and the surface heat and mass flux exponent.

(iv) The phase angles for both heat and mass transfer decrease towards the asymptotic value -45°, while the respective quantity for shear stress reaches the value of -90° in a decreasing manner.

(v) The heat and mass flux exponent parameter n has no significant effects on both amplitude and phase angels as the values of ξ become very large.

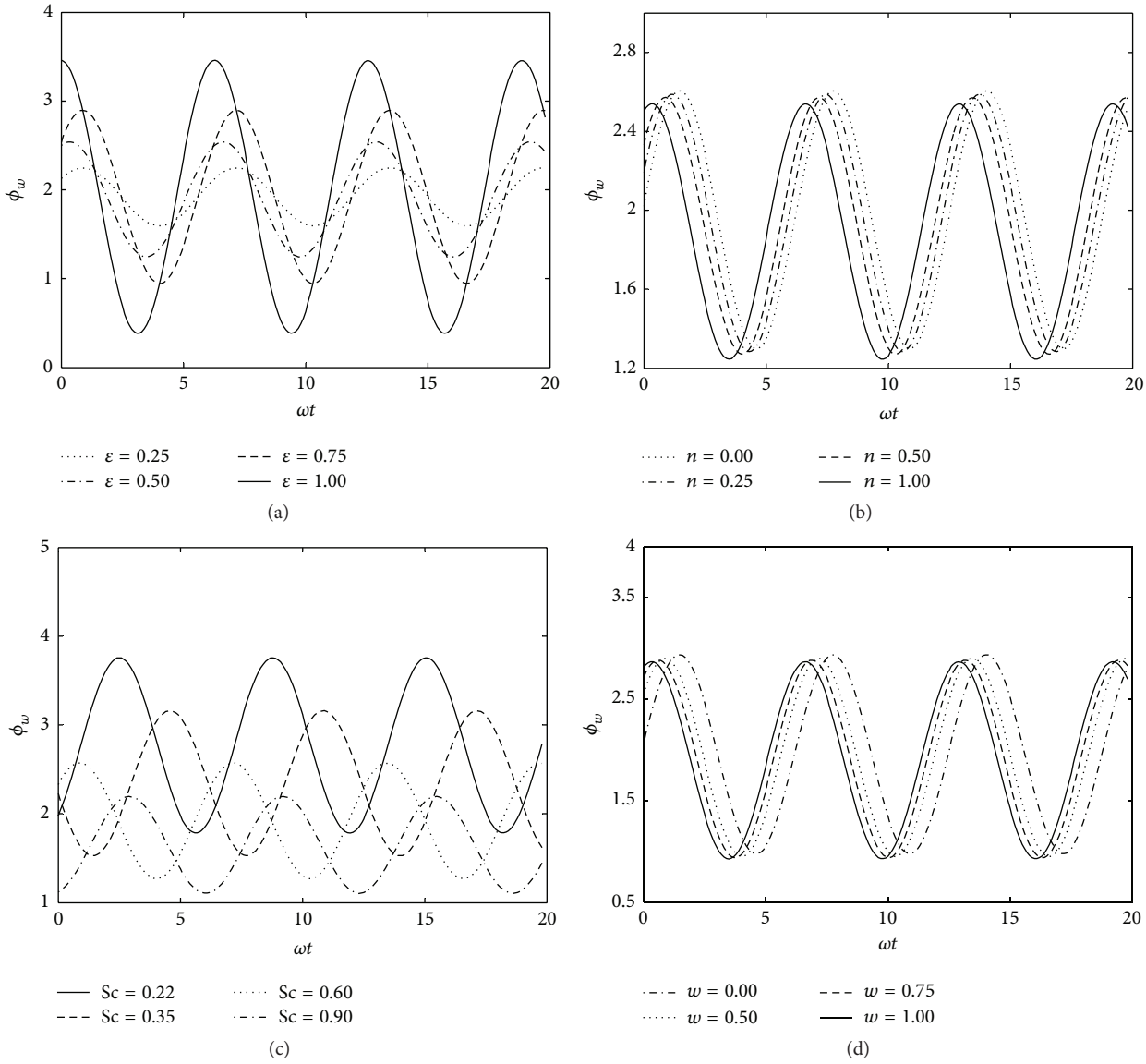

FIGURE 8: Transient surface concentration at $\xi = 1.0$ for different (a) ε, while Pr = 0.7, Sc = 0.6, $w = 0.5$, and $n = 0.5$, (b) n, while Pr = 0.7, Sc = 0.6, and $w = 0.0$, (c) Sc, while Pr = 0.7, $w = 0.5$, and $n = 0.5$, and (d) w, while Pr = 0.7, $n = 0.5$, and Sc = 0.6.

Conflict of Interests

The authors declare that there is no conflict of interests regarding the publication of this paper.

Acknowledgment

Sharmina Hussain would like to take the opportunity to convey her hearty gratitude to the BRAC University authority for granting her Sabbatical Leave for one year during the period of continuing this research.

References

[1] S. Ostrach, "Natural convection with combined driving force," *Physicochemical Hydrodynamics*, vol. 1, pp. 233–247, 1980.

[2] H. E. Huppert and J. S. Turner, "Double diffusive convection," *Journal of Fluid Mechanics*, vol. 106, pp. 299–329, 1981.

[3] A. Bejan, *Convection Heat Transfer*, Wiley, New York, NY, USA, 2nd edition, 1995.

[4] B. Gebhart and L. Pera, "The naturee of vertical natural convection flows resulrting from the combined buoyancy effects of thermal and mass diffusion," *International Journal of Heat and Mass Transfer*, vol. 14, no. 12, pp. 2025–2050, 1971.

[5] A. Mongruel, M. Cloitre, and C. Allain, "Scaling of boundary-layer flows driven by double-diffusive convection," *International Journal of Heat and Mass Transfer*, vol. 39, no. 18, pp. 3899–3910, 1996.

[6] M. J. Lighthill, "The response of laminar skin-friction and heat transfer to fluctuations in the stream velocity," *Proceedings of the Royal Society of London, Series A: Mathematical and Physical Sciences*, vol. 224, no. 1156, pp. 1–23, 1954.

[7] S. Eshghy, V. S. Arpaci, and J. A. Clark, "The effect of longitudinal oscillations on free convection from vertical surfaces," *Journal of Applied Mechanics*, vol. 32, no. 1, pp. 183–191, 1965.

[8] R. S. Nanda and V. P. Sharma, "Free convection laminar boundary layers in oscillatory flow," *Journal of Fluid Mechanics*, vol. 15, no. 3, pp. 419–428, 1963.

[9] P. K. Muhuri and M. K. Maiti, "Free convection oscillatory flow from a horizontal plate," *International Journal of Heat and Mass Transfer*, vol. 10, no. 6, pp. 717–732, 1967.

[10] M. A. Hossain, S. K. Das, and D. A. S. Rees, "Heat transfer response of free convection flow from a vertical heated plate to an oscillating surface heat flux," *Acta Mechanica*, vol. 126, no. 1–4, pp. 101–113, 1998.

[11] M. D. Kelleher and K. T. Yang, "Heat transfer response of laminar free convection boundary-layers along vertical heated plate to surface temperature," *Zeitschrift für angewandte Mathematik und Physik*, vol. 19, pp. 31–44, 1968.

[12] S. Siddiqa, M. A. Hossain, and I. Pop, "Conjugate thermal and mass diffusion effect on natural convection flow in presence of strong cross magnetic field," *International Journal of Heat and Mass Transfer*, vol. 55, no. 19-20, pp. 5120–5132, 2012.

[13] M. A. Hossain, I. Pop, and K. Vafai, "Combined free-convection heat and mass transfer above a near-horizontal surface in a porous medium," *Hybrid Methods in Engineering*, vol. 1, no. 2, pp. 87–102, 1999.

[14] K. R. Khair and A. Bejan, "Mass transfer to natural convection boundary layer flow driven by heat transfer," *Journal of Heat Transfer*, vol. 107, no. 4, pp. 979–981, 1985.

[15] O. V. Trevisan and A. Bejan, "Combined heat and mass transfer by natural convection in a vertical enclosure," *Journal of Heat Transfer*, vol. 109, no. 1, pp. 104–112, 1987.

[16] M. A. Hossain and A. C. Mandal, "Effects of mass transfer and free convection on the unsteady MHD flow past a vertical porous plate with constant suction," *International Journal of Energy Research*, vol. 10, no. 4, pp. 409–416, 1986.

[17] S. Hussain, M. A. Hossain, and M. Wilson, "Natural convection flow from a vertical permeable flat plate with variable surface temperature and species concentration," *Engineering Computations*, vol. 17, no. 7, pp. 789–812, 2000.

[18] M. A. Hossain, S. Hussain, and D. A. S. Rees, "Influence of fluctuating surface temperature and concentration on natural convection flow from a vertical at plate," *Zeitschrift für Angewandte Mathematik und Mechanik*, vol. 81, no. 10, pp. 699–709, 2001.

[19] N. C. Roy and M. A. Hossain, "The effect of conduction-radiation on the oscillating natural convection boundary layer flow of viscous incompressible fluid along a vertical plate," *Proceedings of the Institution of Mechanical Engineers, Part C: Journal of Mechanical Engineering Science*, vol. 224, no. 9, pp. 1959–1972, 2010.

[20] M. K. Jaman and M. A. Hossain, "Effect of uctuations surface temperature on natural convection flow over cylinders of elliptic cross section," *The Open Transport Phenomena Journal*, vol. 2, pp. 35–47, 2010.

[21] S. Hussain, "Computational fluid dynamics study of flow behavior in membrane module with multiple filaments," *BRAC University Journal*, vol. 6, no. 2, pp. 1–10, 2009.

[22] S. Hussain, "CFD study of mass transfer in spacer filled membrane module," *GANIT: Journal of Bangladesh Mathematical Society*, vol. 31, pp. 33–41, 2011.

[23] N. C. Roy, M. A. Hossain, and S. Hussain, "Unsteady laminar mixed convection boundary layer flow near a vertical wedge due to oscillations in the free-stream and surface temperature," *Applications and Applied Mathematics*, In press.

[24] H. B. Keller, "Numerical methods in boundary-layer theory," *Annual Review of Fluid Mechanics*, vol. 10, pp. 417–433, 1978.

[25] J. C. Butcher, "Implicit Runge-Kutta processes," *Mathematics of Computation*, vol. 18, pp. 50–64, 1964.

[26] P. R. Nachtsheim and P. Swigert, "Satisfaction of asymptotic boundary conditions in numerical solution of system of nonlinear equations of boundary layer type," NASA TN D-3004, NASA, 1965.